Langmuir

Article

pubs.acs.org/Langmuir

Molecular Interactions between Lecithin and Bile Salts/Acids in Oils and Their Effects on Reverse Micellization

Ching-Wei Njauw,[†] Chih-Yang Cheng,[†] Viktor A. Ivanov,[‡] Alexei R. Khokhlov,[‡] and Shih-Huang Tung*[,†]

[†]Institute of Polymer Science and Engineering, National Taiwan University, Taipei, 10617 Taiwan

[‡]Faculty of Physics, Moscow State University, Moscow 119991, Russia

Supporting Information

ABSTRACT: It has been known that the addition of bile salts to lecithin organosols induces the formation of reverse wormlike micelles and that the worms are similar to long polymer chains that entangle each other to form viscoelastic solutions. In this study, we further investigated the effects of different bile salts and bile acids on the growth of lecithin reverse worms in cyclohexane and *n*-decane. We utilized rheological and small-angle scattering techniques to analyze the properties and structures of the reverse micelles. All of the bile salts can transform the originally spherical lecithin reverse micelles into wormlike micelles and their rheological behaviors can be described by the single-relaxation-time Maxwell model. However, their efficiencies to induce the worms are different. In contrast, before phase separation, bile acids can induce only short cylindrical micelles that are not long enough to impart viscoelasticity. We used Fourier transform infrared spectroscopy to investigate the interactions between lecithin and bile salts/acids and found that different bile salts/acids employ different functional groups to form hydrogen bonds with lecithin. Such effects determine the relative positions of the bile salts/acids in the headgroups of lecithin, thus resulting in varying efficiencies to alter the effective critical packing parameter for the formation of wormlike micelles. This work highlights the importance of intermolecular interactions in molecular self-assembly.

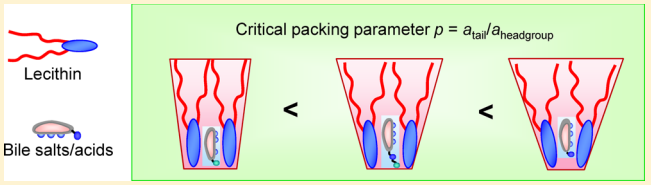

1. INTRODUCTION

It is well known that amphiphilic molecules beyond a critical concentration in water can self-assemble into characteristic structures, such as micelles and vesicles, of diverse shapes and sizes.[1,2] The aqueous self-assembly of amphiphiles is recognized to be driven primarily by hydrophobic interactions (i.e., water molecules revert to a disordered state and gain entropy when the hydrophobes of amphiphilic molecules are buried in the cores of micelles). The self-assembly of amphiphiles can also occur in low-polarity organic liquids ("oils"), and this is referred to as reverse self-assembly.[1,2] Different from aqueous solutions, the driving forces for this type of self-assembly are in general the attractive forces, such as hydrogen bonding interactions, between hydrophilic groups. This effect originated from the tendency of enthalpy toward a minimum. Compared to self-assembly in water, much less is known about reverse self-assembly.[3−12]

Wormlike micelles are cylindrical chains that grow to lengths of several micrometers while maintaining a local flexibility. These micelles can be formed in both water and oils.[13,14] The self-assembly of reverse wormlike micelles in oils has been pioneered by Luisi and co-workers.[15−20] The first examples of such micellar systems were ternary mixtures of lecithin−water−oil.[16] Lecithin is a zwitterionic phospholipid with two hydrocarbon tails (Figure 1), which, when added alone to oil, form reverse spherical or ellipsoidal micelles.[21] When a small quantity of water is added to these fluids, the micelles grow axially into flexible cylinders. The added water is believed to bind lecithin through hydrogen bonds and alters the geometry of the amphiphile to favor the formation of cylinders.[4,21] The growth of these micellar chains and their subsequent entanglements into a transient network transform the sample from a low-viscosity species to a viscoelastic one.[18,20] In turn, the zero-shear viscosity η_0 is enhanced by several orders of magnitude relative to that of neat lecithin solutions. In addition to water, other polar solvents such as formamide, glycerol, and ethylene glycol are also capable of making such a transformation.[22]

Different from conventional liquid additives, bile salts, a class of naturally occurring solid steroidal amphiphiles, have been shown to induce the same effects.[21,23,24] Bile salts are insoluble if directly added to oils but can be solubilized in the presence of lecithin because of intermolecular hydrogen bonds between bile salts and lecithin. Bile salts play a role analogous to that of liquid additives and promote the longitudinal aggregation of lecithin molecules into reverse micellar chains. The molar ratio of bile salt to lecithin (denoted by B_0) is the key parameter in dictating reverse micellar growth. Recently, some more lecithin-based reverse wormlike micellar systems induced by solid substances have been reported.[25−28] In general, the low solubility of additives in oils and strong interactions between additives and lecithin are prerequisite for their addition,

Received: November 18, 2012
Revised: February 24, 2013
Published: February 26, 2013

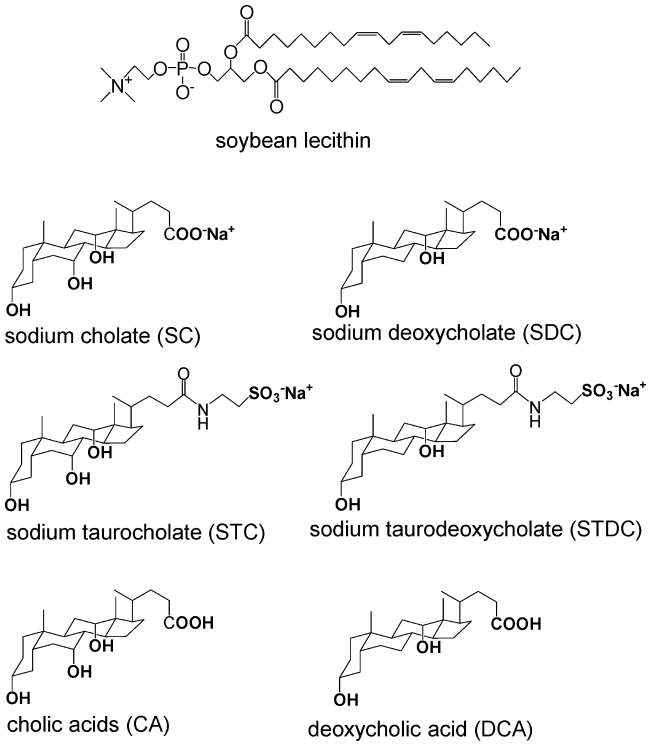

Figure 1. Molecular structures of soybean lecithin, bile salts, and bile acids used in this study.

whether liquid or solid, to induce lecithin reverse worms. Their molecular interactions and resulting arrangements in reverse micelles, however, are still not clear.

In the present study, we conducted a comprehensive investigation on the effects of various bile salts as well as their counterparts—bile acids in oils. The bile salts/acids studied in this work are illustrated in Figure 1. The common feature in the chemical structure of bile salts/acids is a characteristic steroid structure with a rigid, nonplanar fused ring and a carboxylic acid group that may be conjugated with amino acids such as taurine and glycine. Furthermore, different bile salts/acids contain different numbers (one to three) and positions of hydroxyl groups attached to these rings. Because the hydroxyl groups lie on the same side of the ring, bile salts are an unusual class of facial amphiphiles with hydrophilic and hydrophobic faces that are different from those of regular surfactants with hydrophilic heads and hydrophobic tails.[29] Although all of the bile salts/acids are derivatives of steroids and similar in chemical structure, their abilities to induce lecithin reverse worms are significantly different. Because of the similarities in molecular structure, bile salts/acids can serve as model molecules to clarify the role of each main functional group, and this study will demonstrate that the interplays between bile salts/acids and lecithin are crucial for the growth of reverse lecithin micelles.

Lecithin–bile salt interactions are of general interest because of their physiological functions and biomedical applications.[29−34] Bile salts form mixed micelles with lecithin and other lipids in aqueous solutions, and physiologically, the mixed micelles help to emulsify fats in intestines for enzymes to digests the fats.[2,29,30] Also, bile salts have been known to partition into phospholipid bilayers and alter membrane properties, such as the permeability to divalent cations and the surface potential, and may even disrupt cell membranes when their concentration reaches a critical limit.[31−34] In aqueous solutions, the arrangements of lecithin and bile salt in the micelles have been studied by varying methods. Evidence from light scattering,[35] small-angle neutron scattering,[36,37] and HPLC[38] techniques have shown that bile salts and lecithin tend to aggregate into rodlike micelles in water at a certain lecithin–bile salt ratio and concentration. However, the detailed interactions between bile salts and phospholipids are difficult to study because of the disturbance due to the presence of water. The present low-polarity solvents provide a nearly water-free platform to elucidate the strengths and the binding sites of the intermolecular hydrogen bonds. We will show that a slight change in substituent groups on bile salts/acids may greatly influence the intermolecular interaction, and it is such an interaction that determines the molecular arrangements in oils and thus regulates the reverse self-assembly behavior.

2. EXPERIMENTAL SECTION

2.1. Materials. Soybean lecithin (95% purity) containing 97.2 wt % phosphatidylcholine and 2.8 wt % lysophosphatidylcholine was purchased from Avanti Polar Lipids, Inc. The fatty acid distribution of the lecithin is shown in Figure S1 in the Supporting Information, mostly consisting of those with 18 carbons with 2 double bonds, as drawn in Figure 1. The bile salts—sodium cholate (SC, >99%), sodium deoxycholate (SDC, >97%), sodium taurocholate (STC, >97%), and sodium taurodeoxycholate (STDC, >95%)—and the bile acids, cholic acids (CA, >98%), and deoxycholic acid (DCA, >99%) were purchased from Sigma-Aldrich. Cyclohexane (>99.5%) and *n*-decane (>99%) were purchased from J. T. Baker and Alfa-Aesar, respectively. Deuterated cyclohexane (99.5% D) was obtained from Cambridge Isotopes.

2.2. Sample Preparation. Bile salts and bile acids are insoluble in cyclohexane and *n*-decane. To facilitate sample preparation, they were first premixed with lecithin in methanol, a common solvent for all of the chemicals. Lecithin, bile salts, and bile acids were dissolved in methanol to form 200, 100, and 100 mM stock solutions, respectively. Samples of the desired composition were prepared by mixing the stock solutions. Methanol was removed by drying in a vacuum oven at 50 °C for 48 h, and solid mixtures of lecithin and bile salts/acids were formed. The final samples with the desired concentrations were obtained by adding cyclohexane or *n*-decane to the solid mixtures, followed by stirring until the solutions became transparent and homogeneous. The above procedure also ensured the elimination of removable residual water from the sample and thereby facilitated reproducible sample preparation. Samples were equilibrated for at least 3 days before measurements.

2.3. Rheological Studies. Steady and dynamic rheological experiments were performed on an AR2000EX stress-controlled rheometer (TA Instruments). Samples were run on cone-and-plate geometries (40 mm diameter/4° cone angle). The plates were equipped with a Peltier-based temperature control, and all samples were studied at 25 ± 0.1 °C. A solvent trap was used to minimize the evaporation of solvent. Dynamic frequency spectra were conducted in the linear viscoelastic regime of the samples, as determined from dynamic strain sweep measurements. For steady-shear experiments, sufficient time was allowed before data collection at each shear rate to ensure that the viscosity reached its steady-state value.

2.4. Small-Angle Neutron and X-ray Scattering (SANS and SAXS). SANS measurements were made on the NG-7 beamline at NIST in Gaithersburg, MD. Neutrons with a wavelength of 6 Å were selected. Two sample–detector distances, 1.3 and 13.2 m, were used to obtain data over a range of wave vector q from 0.004 to 0.4 Å^{-1}. Deuterated cyclohexane (*d*-cyclohexane) instead of protonated cyclohexane was used as the solvent to enhance the scattering contrast. Scattering spectra were corrected and placed on an absolute scale using NIST calibration standards. SAXS measurements were conducted on the BL23A1 beamline at the National Synchrotron Radiation Research Center (NSRRC), Taiwan.[39] A monochromatic

dx.doi.org/10.1021/la304601p | *Langmuir* 2013, 29, 3879−3888

beam of λ = 1.240 Å was used. The scattering patterns were collected on a Mar-CCD with a diameter of 165 mm over a q range from 0.007 to 0.3 Å^{-1}. Samples were studied at 25 °C. The data are shown as plots of the absolute intensity I versus $q = 4\pi \sin(\theta/2)/\lambda$, where λ is the wavelength and θ is the scattering angle.

2.5. SANS and SAXS Modeling. Modeling of SANS and SAXS data was conducted using the analysis package provided by NIST with IGOR Pro software.[40] For dilute solutions of noninteracting scatterers, the SANS or SAXS intensity $I(q)$ can be modeled in terms of the form factor $P(q)$ of the scatterers

$$I(q) = c\Delta\rho^2 P(q) + B \tag{1}$$

where c is the total concentration, $\Delta\rho$ is the excess scattering length density, and B is the background. In this study, we consider form factor models for flexible cylinders. The form factor for semiflexible chains of contour length L, Kuhn length b, and cross-sectional radius R can be represented as the product of cross-sectional form factor P_{CS} and wormlike chain form factor P_{WC}:[41,42]

$$P(q) = P_{CS}(q, R)\, P_{WC}(q, L, b) \tag{2}$$

The cross-sectional form factor P_{CS} can be approximated by the following expression, which is valid for cylindrical chains,

$$P_{CS}(q, R) = \left[\frac{2J_1(qR)}{qR}\right]^2 \tag{3}$$

where $J_1(x)$ is the first-order Bessel function given by

$$J_1(x) = \frac{\sin x - x\cos x}{x^2} \tag{4}$$

For cylinders with a polydisperse radius, the form factor should be averaged over the radius distribution in the following manner

$$P_{CS}(q, R_0) = \int f(R)\, P_{CS}(q, R)\, dR \tag{5}$$

where R_0 is the average cylinder radius. The polydispersity in cylinder radius $f(R)$ is accounted for by a Schulz distribution

$$f(R) = \left(\frac{z+1}{R_0}\right)^{z+1} \frac{L^z}{\Gamma(z+1)} \exp\left(-(z+1)\frac{R}{R_0}\right) \tag{6}$$

where Γ is the gamma function and z is a parameter related to the width of the distribution. The polydispersity index p_d is given by

$$p_d = \frac{1}{\sqrt{z+1}} \tag{7}$$

The form factor P_{WC} for a wormlike chain with excluded-volume interactions is detailed in the paper by Pedersen and Schurtenberger,[42] where it was originally derived, and then modified by Chen et al.[43] The parameters used in the fitting procedures included c, L, b, R, p_d, $\Delta\rho$, and B.

2.6. Fourier Transform Infrared Spectra (FT-IR). FT-IR spectra were recorded in transmission mode with a PerkinElmer Spectrum 100 model FT-IR spectrometer. Liquid samples of 100 mM lecithin with 30 mM bile salts/acids in cyclohexane were loaded into a CaF_2 cell (0.05 mm thickness) and analyzed over a range of wavenumbers from 4000 to 1000 cm^{-1} at 25 °C. Each spectrum was collected under an accumulation of 16 scans at 1 cm^{-1} resolution. Pure solvents in the CaF_2 cell were taken as background references before measuring sample spectra.

3. RESULTS AND DISCUSSION

3.1. Rheology. We first focus on the rheological behavior of lecithin−bile salts/acids in n-decane. Figure 2 shows the zero-shear viscosity η_0 of solutions containing 100 mM lecithin and various concentrations of four bile salts in n-decane at 25 °C, where B_0 is the molar ratio of bile salts to lecithin. The values of η_0 were obtained from steady-shear rheological experiments in the limit of low shear rates. For all four bile salts, η_0 increases dramatically as B_0 increases. All of these solutions are transparent and isotropic below a critical ratio B_0^{max}. At B_0^{max}, η_0 reaches its maximum and samples flow very slowly in inverted vials because of their high viscosity. Above B_0^{max}, samples phase separate into two isotropic liquid phases, one nonviscous and the other viscous. The lower, viscous phase contains most of the lecithin and bile salts, and the upper, nonviscous phase is a dilute solution. Similar behavior can be found in cyclohexane, as shown in Figure S2 in the Supporting Information.

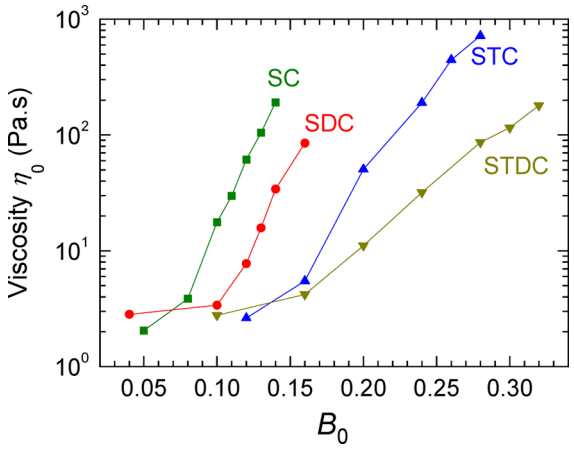

Figure 2. Zero-shear viscosity η_0 of lecithin−bile salt mixtures in n-decane at 25 °C as a function of B_0, the molar ratio of bile salts to lecithin, with the lecithin concentration held constant at 100 mM. For all of the bile salts, the viscosity increases dramatically with B_0 until B_0^{max} is reached, where the sample flows very slowly in the overturned vial. After B_0^{max}, the sample phase separates into two coexisting liquid phases. Note that the efficiency to enhance viscosity is in the order of SC > SDC > STC > STDC.

The viscoelasticity of lecithin−bile salt samples was characterized by dynamic rheology. Figure 3 shows the dynamic rheological data (i.e., elastic modulus G' and viscous modulus G'') as functions of frequency ω for samples containing 100 mM lecithin at B_0^{max} for the four bile salts at 25 °C. The data clearly reveal the viscoelastic response of these four samples. At high ω or short time scales, the samples show elastic behavior, with G' approaching a plateau and dominating G''. On the other hand, at low ω or long time scales, the samples show viscous behavior, with G'' exceeding G' and the slopes of G' and G'' being close to 2 and 1, respectively, on the log−log plot. In Figure 3, we also show fits to $G'(\omega)$ and $G''(\omega)$ using a Maxwell model with a single relaxation time:[44]

$$G'(\omega) = \frac{G_p \omega^2 t_R^2}{1 + \omega^2 t_R^2} \tag{8}$$

$$G''(\omega) = \frac{G_p \omega t_R}{1 + \omega^2 t_R^2} \tag{9}$$

Here, G_p is the plateau modulus (i.e., the value of G' in the high-frequency limit). The Maxwell model fits the data reasonably well at low and intermediate frequencies, but there is a discrepancy at high frequencies, which has been attributed to the effect of a more rapid Rouse motion. This confirms that a single relaxation time dominates the rheological response of these samples. The dominant relaxation time t_R of these viscoelastic samples can be estimated as $1/\omega_c$, where ω_c is

dx.doi.org/10.1021/la304601p | Langmuir 2013, 29, 3879−3888

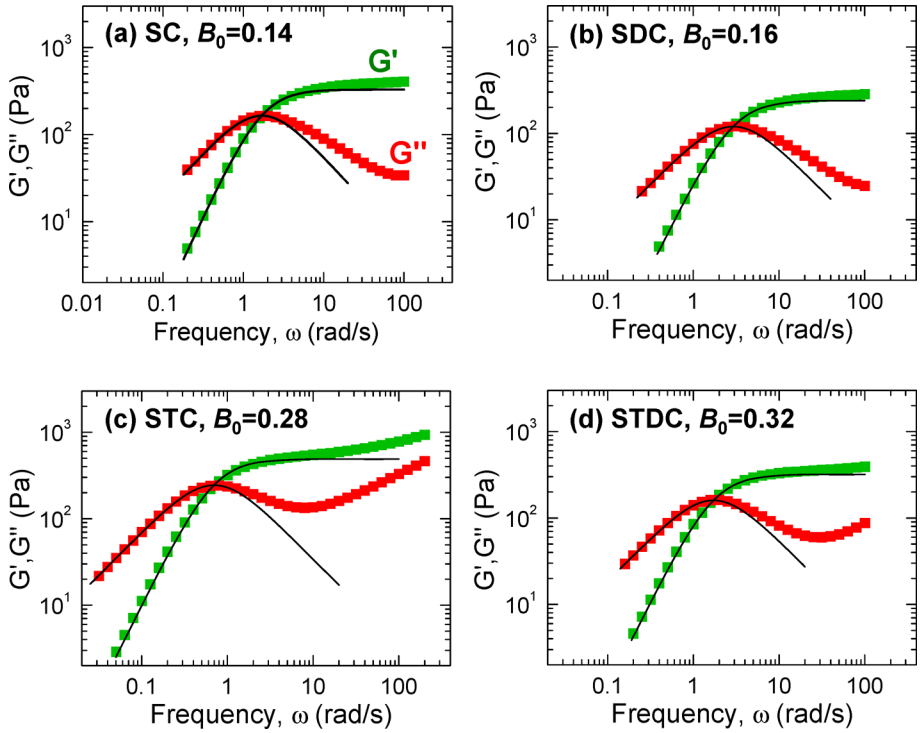

Figure 3. Dynamic rheology of lecithin−bile salt mixtures in *n*-decane at 25 °C. The samples contain 100 mM lecithin at the B_0^{max} of each bile salt. The plots show the elastic modulus G' and viscous modulus G'' as functions of frequency ω. Fits to a single-relaxation-time Maxwell model are shown as solid lines.

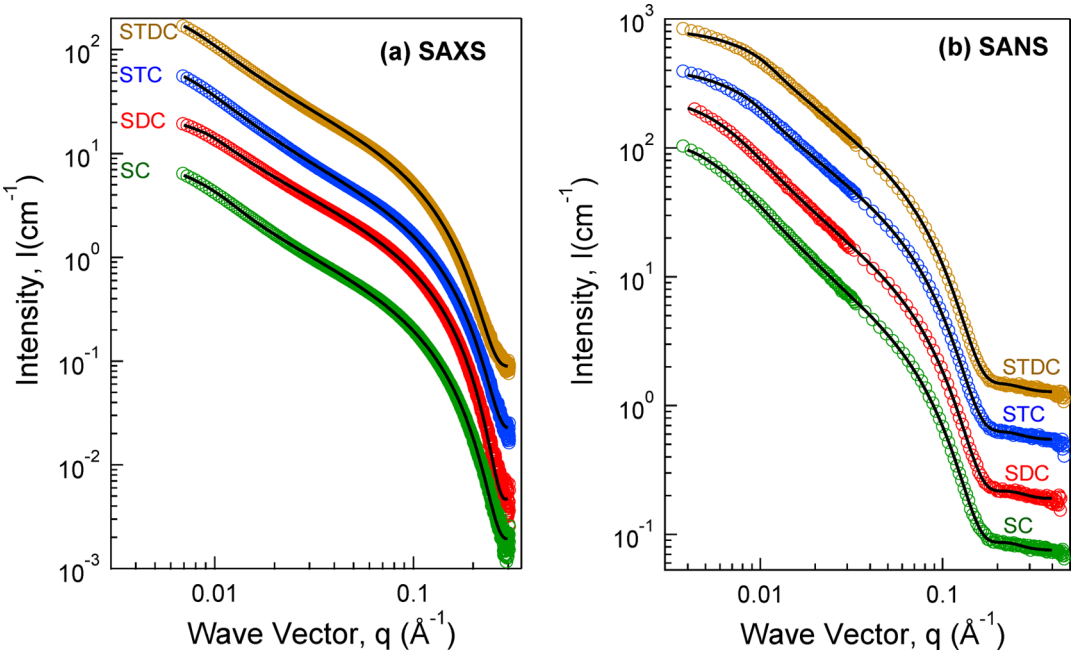

Figure 4. (a) SAXS and (b) SANS spectra for lecithin−bile salt mixtures in protonated and deuterated cyclohexane, respectively, at 25 °C. The lecithin concentration is 20 mM in all samples. B_0 values for SC, SDC, STC, and STDC are 0.4, 0.4, 0.7, and 0.7, respectively. Model fits are shown as solid lines through each data curve.

the frequency at which G' and G'' cross. Maxwell fluidlike behavior is indicative of entangled wormlike micelles.[44] The viscoelastic behaviors of lecithin−bile salt reverse worms in cyclohexane are shown in Figure S3 in the Supporting Information.

In Figure 2, an interesting observation is that B_0^{max} values of the four bile salts are different, in increasing order 0.14, 0.16, 0.28, and 0.32 for SC, SDC, STC, and STDC, respectively. The B_0^{max} values of the bile salts bearing a taurine group (STC and STDC) are about twice as high as those without taurine (SC and SDC), and the values of cholic-type salts are slightly smaller than those of deoxycholic-type salts. We also mixed lecithin with bile acids CA and DCA in *n*-decane. However, the viscosity was only slightly increased to ∼0.5 Pa·s, and the

dx.doi.org/10.1021/la304601p | *Langmuir* 2013, 29, 3879−3888

Table 1. Parameters from SAXS and SANS Modeling of Lecithin−Bile Salt Samples

	av radius R_0 (Å)		polydispersity p_d		Kuhn length b (Å)		Contour length L (Å)	
sample (B_0)	SAXS	SANS	SAXS	SANS	SAXS	SANS	SAXS	SANS
SC (0.4)	13.1	20.2	0.12	0.17	280.9 ± 0.3	218.3 ± 1.6	946.7 ± 1.7	1720.0 ± 11.3
SDC (0.4)	13.2	19.7	0.10	0.16	333.3 ± 0.4	251.8 ± 2.2	694.7 ± 1.1	1386.4 ± 10.0
STC (0.7)	12.7	19.6	0.10	0.18	230.6 ± 0.2	349.5 ± 2.4	1278.6 ± 3.4	789.6 ± 3.5
STDC (0.7)	13.1	19.5	0.14	0.18	276.5 ± 0.3	317.4 ± 2.2	1174.9 ± 3.7	638.3 ± 2.7

samples were still liquid-like, even though the B_0^{max} values of CA and DCA, 0.32 and 0.46, respectively, are higher than those of bile salts. Very similar results were obtained in cyclohexane, $B_0^{max} \approx 0.4$, 0.45, 0.8, and 0.85 for SC, SDC, STC, and STDC, respectively.[21] The difference is that the B_0^{max} values in cyclohexane are larger than those in *n*-decane, which has been a general observation in all lecithin-based wormlike micellar systems. The different B_0^{max} values for bile salts/acids are associated with the strengths of intermolecular interactions and will be discussed in the FT-IR section.

Figure 2 also reveals that the efficiencies of the four bile salts in inducing the formation of wormlike micelles are quite different, in the order of SC > SDC > STC > STDC. When the viscosities of SC and SDC samples reach their maxima, STC and STDC samples are still low-viscosity liquids. It has been shown that the growth of lecithin micelles induced by bile salts is caused by the change in effective molecular geometry as a result of the fact that bile salts insert into lecithin headgroups and consequently expand headgroup areas while tail areas remain unchanged.[21] Following this argument, cholic-type salts, which contain one more hydroxyl group on the steroid ring and thus possess larger molecular volumes, are reasonably more efficient than deoxycholic-type salts. However, it is puzzling that the taurine-based bile salts are less efficient at inducing wormlike micelles, taking into account that the molecular volumes of taurine-based bile salts are larger than those of the bile salts without taurine. Furthermore, it is still mysterious that bile acids can lead only to short cylindrical micelles that are unable to impart viscoelasticity before phase separation, considering that the chemical structures of bile acids are so similar to those of corresponding bile salts. A more detailed mechanism based on where exactly bile salt/acid molecules are incorporated into the headgroups of lecithin will be provided to explain these phenomena and will be discussed later in this Article.

3.2. SAXS and SANS. SAXS and SANS experiments were performed on lecithin−bile salt solutions to elucidate micellar structures. SAXS data were obtained using protonated cyclohexane as the solvent, and SANS data were obtained using deuterated cyclohexane, both at 25 °C. The lecithin concentration was fixed at 20 mM, and the values of B_0 selected for the measurements were 0.4, 0.4, 0.7, and 0.7 for SC, SDC, STC, and STDC, respectively, which are near B_0^{max} of each bile salt in cyclohexane to ensure the formation of wormlike micelles.[21] $I(q)$ plots are shown in Figure 4, and the intensities of the plots are rescaled for clarity. SAXS (Figure 4a) and SANS (Figure 4b) data of all four bile salts show a power-law behavior close to $I \approx q^{-1}$ (slope of −1 on the log−log plot) at intermediate q, which is the scaling relationship expected for cylindrical structures.[41]

We have fitted a form-factor model for flexible cylinders with a polydisperse radius to the SAXS and SANS data, and the fits are shown in Figure 4 as solid lines through the data. Both SAXS and SANS data could be well fit by the model, indicating the presence of wormlike micelles in the solutions. The slight discrepancy at low q for SANS data could be due to the polydispersity of the contour length of worms. The parameters from the modeling are shown in Table 1. From the fit parameters, the radii of the wormlike micelles induced by different bile salts are nearly the same but the values obtained from SAXS, ∼13 Å, are smaller than those from SANS, ∼20 Å. The overlap of SAXS and SANS curves in the high-q range shown in Figure S4 in the Supporting Information confirms the very similar radii of the worms.

The scattering of X-rays arises from the interactions of incident X-rays with electrons in samples. Thus, SAXS measurements reflect the contrast of electron density between scatters and their surroundings, which, in the present case, is presumably the contrast between the hydrophilic headgroups (with bound bile salts) and the hydrophobic hydrocarbon tails of lecithin. The independence of the radius on the types of bile salts implies that bile salt molecules are mostly distributed within lecithin headgroups. In contrast, neutrons are scattered by atomic nuclei in samples so that SANS intensity profiles result from the contrast between the hydrogen atoms on lecithin/bile salts and the heavier deuterium atoms on the solvent (i.e., *d*-cyclohexane in the present study). Cyclohexane is excluded from the hydrophilic headgroups and may only penetrate and swell the outer portion of lecithin tails, which explains why the radii measured from SANS are larger. It has been shown that as the micelles grow upon addition of bile salt (SDC) from oblate ellipsoids to cylinders and then to worms, the cylinder radius remains constant and identical to that of the minor axis of the oblate,[21] unlike the addition of salts with multivalent cations such as Ca^{2+} and La^{3+}, which effectively forces the tails into a more straightened conformation and gives rise to an increase in the cylinder radius.[9] Similar radii from SANS indicate that the bile salts have no significantly different effects on the conformation of lecithin tails. The Kuhn length b shown in Table 1 is in the range of 200−350 Å, which is consistent with the values from the Holtzer (or bending rod) plot, as shown in Figure S5 in the Supporting Information. The larger contour lengths L compared to Kuhn lengths imply that the cylindrical micelles are flexible.

3.3. FT-IR. SAXS data suggest that bile salts are bound in headgroup areas of lecithin. The interactions between lecithin and bile salts, more specifically, the hydrogen bonding interactions, must play an important role in the structural transformation. The interplay between lecithin and bile salts has been widely studied in aqueous solutions because of the physiological importance. Now we focus on oil systems and the interactions were studied using FT-IR. It has been shown that the primary sites on lecithin headgroups for forming hydrogen bonds are the phosphate groups (OPO^-).[45] The frequency of asymmetric phosphate stretching on lecithin in low-polarity organic solvents is near 1260 cm^{-1}, and the band shifts to lower frequency (i.e., a red shift) when hydrogen bonded.[45,46] Figure 5 shows the FT-IR spectra in the range of 1300−1200 cm^{-1} for

dx.doi.org/10.1021/la304601p | Langmuir 2013, 29, 3879−3888

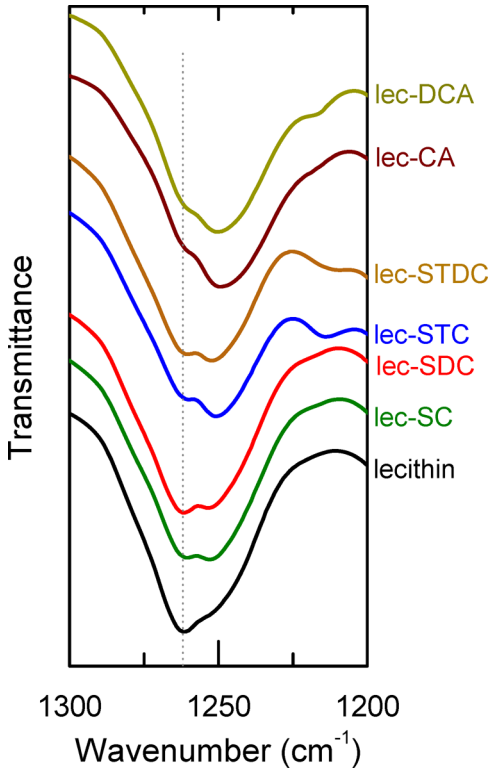

Figure 5. FT-IR absorption bands of phosphate groups (OPO^-) on lecithin for lecithin−bile salt/acid mixtures in cyclohexane at 25 °C. The lecithin concentration is 100 mM, and B_0 is 0.3 for all of the bile salts/acids.

samples with 100 mM lecithin and 30 mM bile salts or bile acids (B_0 = 0.3) in cyclohexane. Pure lecithin in cyclohexane shows a phosphate absorption band at 1261 cm^{-1}. A shoulder at around 1250 cm^{-1} is the signal of phosphate groups hydrogen bonded with a trace of bound water that cannot be removed by drying.[21] When mixed with bile salts and bile acids, in addition to the 1261 cm^{-1} band, absorption bands of hydrogen-bonded phosphate groups become pronounced. The peak positions are 1253, 1253, 1251, 1252, 1249, and 1250 cm^{-1} for SC, SDC, STC, STDC, CA, and DCA, respectively. Because of the low B_0 of 0.3, only partial phosphate groups are hydrogen bonded. This is why the 1261 cm^{-1} band of non-hydrogen-bonded groups can still be seen. Comparing the absorption areas of the two bands, the 1261 cm^{-1} band is still notable for SC and SDC whereas it diminishes and instead the hydrogen-bonded band dominates the absorption for STC, STDC, CA, and DCA samples.

The changes in the peak positions and the absorption areas suggest that the strengths of hydrogen-bonding interactions of DA and DCA are the strongest, followed by those of STC and STDC, and those of SC and SDC are the weakest. The carboxylic acids on DA and DCA and the amide groups on STC and STDC are strong hydrogen-bond donors. Therefore, CA and DCA form stronger hydrogen bonds with phosphate groups on lecithin primarily through the carboxylic acids while STC and STDC do so through the amide groups. For SC and SDC, the hydroxyl groups on the steroid rings are the only weak hydrogen-bond donors, and thus the changes in the FT-IR bands are the smallest. The strength of hydrogen-bonding interactions explains the observation that a greater amount of bile acids (CA and DCA) and taurine-based bile salts (STC and STDC) can be incorporated into lecithin solutions than those of SC and SDC before phase separation, as the trend in B_0^{max} values shown in Figure 2. The functional groups on bile salts and bile acids that form hydrogen bonds with lecithin and their relative positions are depicted in Figure 8.

In addition to phosphate groups, the carbonyl groups (C═O) on lecithin may form hydrogen bonds with bile salts or bile acids. The stretching frequency of C═O groups on lecithin in low-polarity organic solvents is near 1740 cm^{-1}.[45,46] In the widely studied lecithin−water−oil systems, it has been shown that this absorption band shifts to lower frequency because of the formation of hydrogen bonds with water. However, the shift is small compared to that of phosphate stretching bands, and marked shifts are detected only at high water/lecithin molar ratios w_0. It has been concluded that the hydrogen bonds between water and C═O are relatively weak and water molecules interact with C═O only after the phosphate groups are fully hydrated. Returning to the present systems, FT-IR data in the range of 1770−1710 for lecithin−bile salt/acid samples with B_0 = 0.3 are shown in Figure 6. Pure lecithin in

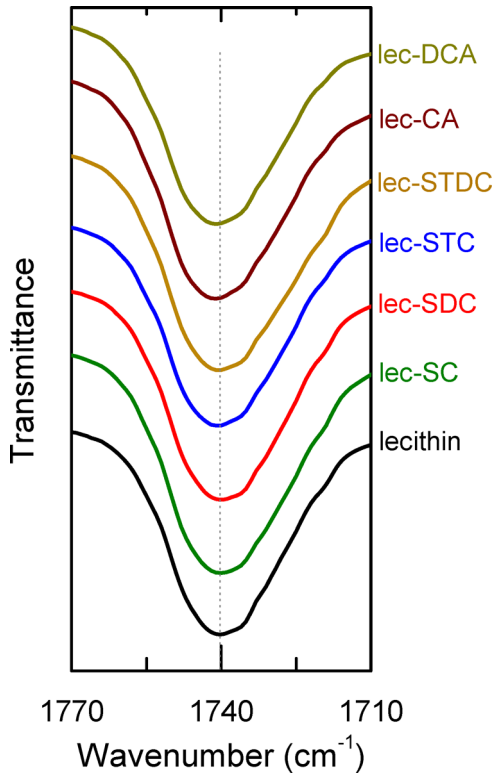

Figure 6. FT-IR absorption band of carbonyl group C═O on lecithin for lecithin−bile salt/acid mixtures in cyclohexane at 25 °C. The lecithin concentration is 100 mM, and B_0 is 0.3 for all of the bile salts/acids. The bands are slightly blue-shifted for STC, STDC, CA, and DCA mixtures.

cyclohexane gives a C═O stretching band at 1740 cm^{-1}. When mixed with SDC and SC, the bands are unchanged. However, although the changes are very small, we could consistently observe that the maximum absorptions appear between 1740 and 1741 cm^{-1} for STC and STDC and at 1741 cm^{-1} for CA and DCA (i.e., a blue shift for taurine-based bile salts and bile acids). Opposite to the red shift in lecithin−water−oil systems, the bands remain the same or even shift to higher frequency in the present systems.

dx.doi.org/10.1021/la304601p | Langmuir 2013, 29, 3879−3888

Pure lecithin in low-polarity organic solvents, such as cyclohexane, has been shown to form reverse spherical micelles where lecithin molecules are organized in a closely packed manner.[21] In such a micellar state, there would be an intermolecular dipole−dipole interaction between C═O groups, which would lead to a red shift of the C═O stretching bands.[47] In other words, the band of C═O stretching observed in cyclohexane (i.e., 1740 cm^{-1} shown in Figure 6) is not the band of isolated lecithin molecules. To examine the interactions of lecithin molecules in an isolated form, we used methanol as a solvent in which lecithin molecules would not aggregate if the concentrations were not particularly high. The FT-IR data of 100 mM lecithin in methanol are shown in Figure 7. The

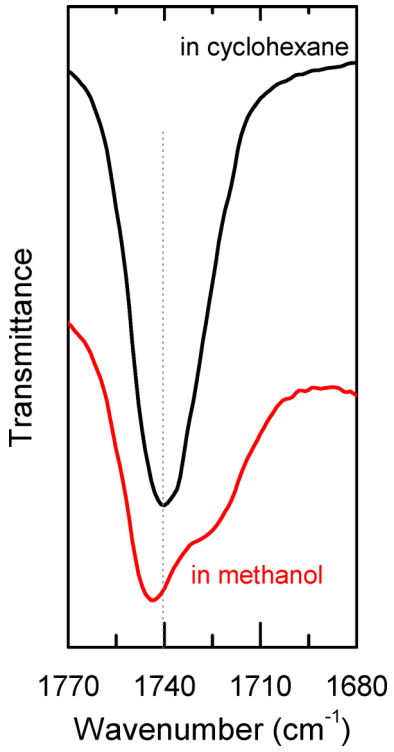

Figure 7. Comparison of the FT-IR absorption bands of carbonyl group C═O on lecithin in methanol and cyclohexane at 25 °C. The lecithin concentration is 100 mM.

maximum in the C═O absorption profile appears at 1744 cm^{-1}, which is higher than that in cyclohexane. Although lecithin is capable of forming hydrogen bonds with the hydroxyl group on methanol, methanol molecules prefer to form hydrogen bonds with other methanol molecules rather than with lecithin molecules.[48] Thus, the 1744 cm^{-1} band can be reasonably assigned to the isolated lecithin molecules that are not hydrogen bonded, and the shoulder around 1725 cm^{-1} is the absorption given by a small number of lecithin molecules hydrogen bonded to methanol.

Back to the lecithin−bile salt/bile acid cases, the unchanged C═O bands in SC and SDC mixtures indicate that SC and SDC have trivial effects on the C═O groups of lecithin. The blue shifts for STC, STDC, CA, and DCA, however, imply a net effect of isolation of lecithin molecules. In other words, STC, STDC, CA, and DCA molecules insert between C═O groups and work as a spacer to separate lecithin molecules. The separation effect dominates the weak hydrogen-bonding interactions between C═O groups and bile salts/acids that are supposed to cause a red shift. Moreover, the FT-IR data in Figure 6 reveal that such separation effects are more pronounced for bile acids (DA and DCA) than for taurine-based bile salts (STC and STDC). The FT-IR results provide important information about the mechanism for the formation of lecithin reverse worms as described below.

3.4. Mechanism. We now have a clearer picture about how bile salts/acids interact with lecithin so as to explain the counterintuitive micellization behavior: (i) larger taurine-based bile salts (STC and STDC) are less efficient at inducing long wormlike micelles and (ii) similarly structured bile acids (CA and DCA) are unable to induce long-enough wormlike micelles to cause viscoelasticity. As interpreted from the FT-IR data shown in Figure 5, STC and STDC make use of amide groups whereas CA and DCA employ carboxylic acids to form hydrogen bonds with phosphate groups on lecithin, which means that the steroid rings on these four molecules insert more deeply into the lecithin tails than do those of SC and SDC, whose hydrogen bond donors are on the steroid rings. This argument is supported by the blue shift of lecithin C═O bands in STC, STDC, CA, and DCA samples shown in Figure 6 as a result of the insertion of steroid rings that separate C═O groups. In contrast, the steroid rings of SC and SDC are restricted around the phosphate groups by hydrogen bonds, and thus the molecules are located mostly on the very end of lecithin headgroups. The relative positions of lecithin−bile salts/acids are depicted in Figure 8.

It is known that the shape of the self-assembled structure formed by amphiphiles is governed by the effective molecular geometry, which can be simply expressed by the critical packing parameter $p = v_{tail}/a_{hg}l_{tail}$, where v_{tail} is the tail volume, a_{hg} is the headgroup area, and l_{tail} is the tail length. The ratio v_{tail}/l_{tail} can be converted to tail area a_{tail}, namely, $p = a_{tail}/a_{hg}$.[1,49] In organic solvents, the formation of reverse micelles requires a packing parameter p well in excess of 1, and for reverse spherical micelles to grow into reverse cylindrical micelles, the packing parameter p must decrease. All of the bile salts and bile acids can bind the phosphate groups of lecithin and increase the headgroup area a_{hg}, thus leading to a net effect of decreasing p. Their efficiencies to decrease p, however, are dependent on the location of bile salts/acids relative to lecithin. In the cases of SC and SDC, bile salt molecules concentrate in the areas next to the phosphate and choline groups of lecithin (Figure 8). a_{hg} is largely increased whereas a_{tail} is maintained about the same and thus p decreases quickly with increasing amounts of SC and SDC. For STC and STDC, the molecules are longer and the amide groups form hydrogen bonds with the phosphate groups so that their steroid rings are extended into the glycerol ester areas. Although a_{hg} is increased, a_{tail} is also slightly increased. In other words, the efficiency to decrease p is lower than that of SC and SDC, and this is why more STC and STDC is required to reach the viscosity maximum. Note that the missing OH of STDC is the one in the middle of the steroid rings, not the one on the end. The OH group at this position may still increase a_{hg} more than a_{tail} so that STC is more efficient than STDC. Following the same argument, bile acids CA and DCA, which are mostly distributed around the areas of phosphates and glycerol esters so that they are less able to expand the choline areas, are supposed to have very low efficiencies to decrease p, and this is the reason that they are unable to induce sufficiently long wormlike micelles before phase separation.

The findings in this work inspired us to answer an unsolved problem in the widely studied lecithin−water−oil reverse

dx.doi.org/10.1021/la304601p | Langmuir 2013, 29, 3879−3888

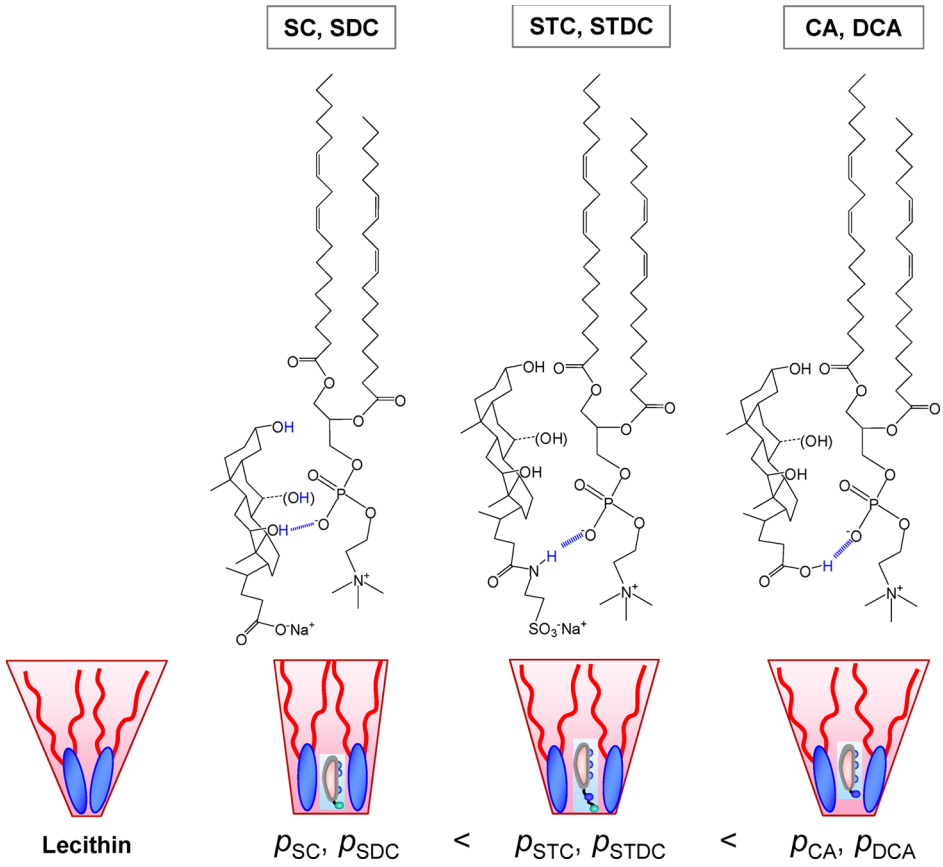

Figure 8. Schematic of hydrogen bonds formed between lecithin and bile salts/acids and the relative molecular positions in oils. Lecithin is shown as a molecule with a blue head and two red tails, and the bile salts/acids are schematically represented as facial amphiphiles. When bile salts/acids bind to the lecithin headgroups, their positions relative to lecithin are dependent on the groups that form hydrogen bonds. SC and SDC are more efficient at expanding headgroup areas whereas STC, STDC, CA, and DCA are less efficient because of their steroid rings inserting into the areas of glycerol esters on lecithin. Here, p is the critical packing parameter.

wormlike micellar systems. It has been shown that when water is added to a lecithin organosol, the viscosity increases to a maximum at a certain water/lecithin molar ratio w_0^{max} whereas further addition of water typically causes a decrease in viscosity, followed by phase separation.[18,20] This is qualitatively different from the behaviors with bile salts. Such a phenomenon has been correlated with the formation of branched wormlike micelles above w_0^{max}, as inferred from the scaling dependences of rheological parameters.[50] FT-IR studies, however, may tell another story. Previous FT-IR studies have shown that water molecules initially prefer to bind phosphate groups of lecithin and the viscosity dramatically increases with w_0, and after phosphates groups are completely hydrated, excess water molecules begin to interact with C═O groups. Coincidently, the shift of the C═O stretching band becomes noticeable when the samples experience a significant decrease in viscosity.[45,46] On the basis of those reported FT-IR results and the support from the present study, we would like to suggest an alternative explanation: above w_0^{max}, because of the insertion of excess water molecules into the glycerol ester area, a_{tail} is increased while a_{hg} is fixed at the fully hydrated level and thus p is increased, which in turn gives rise to a gradual transformation of the long wormlike micelles back to shorter ones. Therefore, a decrease in viscosity is observed.

4. CONCLUSIONS

In this study, various bile salts and acids were incorporated into lecithin organosols, and the efficiency to induce reverse wormlike micelles from high to low was found to be regular bile salts (SC and SDC), taurine-based salts (STC and STDC), and then bile acids (CA and DCA). We have demonstrated that the positions of the primary groups on bile salts/acids that form hydrogen bonds with lecithin are the key to modulating the self-assembly. Although bile acids and taurine-based bile salts interact more strongly with lecithin and taurine-based bile salts are even larger in size, they are less efficient at inducing reverse worms compared to regular bile salts. This is because in order to form the most stable hydrogen bonds, bile acid and taurine-based bile salt molecules must go deeply into the glycerol ester areas of lecithin, which, in terms of the critical packing parameter, reduces the net effect of expanding effective headgroup areas, and thus the tendency to form long worms is prohibited. This work successfully correlates molecular interactions with molecular self-assemblies and also rheological behavior. Although they were focused on oil systems, the experimental methods and the results shown here may inspire research into biomolecular interactions as well as serve as a guideline for the self-assembly of amphiphiles.

dx.doi.org/10.1021/la304601p | *Langmuir* 2013, 29, 3879−3888

■ ASSOCIATED CONTENT

Supporting Information

Fatty acid distribution of lecithin, steady shear and dynamic rheological data of lecithin + bile salts in cyclohexane, overlapped SAXS and SANS data, and Holtzer plot of SANS data. This material is available free of charge via the Internet at http://pubs.acs.org/.

■ AUTHOR INFORMATION

Corresponding Author

*E-mail: shtung@ntu.edu.tw.

Notes

The authors declare no competing financial interest.

■ ACKNOWLEDGMENTS

This work was financially supported by a joint grant from the Taiwan National Science Council (NSC 99-2923-E-002-003) and the Russian Foundation for Basic Research (RFBR 10-03-92003). We acknowledge NSRRC, Taiwan, for facilitating the SAXS experiments and for sponsoring the travel expense of SANS experiments (2011-2-161-1). We thank NIST NCNR, USA, for facilitating the SANS experiments performed as part of this work. The assistance with scattering experiments from Dr. Chun-Jen Su, Dr. Chun-Yu Chen, and Dr. U-Ser Jeng of NSRRC is acknowledged. Helpful discussions on SANS experiments and modeling with Dr. Wei-Ren Chen of ORNL, USA, are also acknowledged. S.-H.T.'s views on wormlike micelles have been shaped by Prof. Srinivasa R. Raghavan of the University of Maryland, College Park, MD.

■ REFERENCES

(1) Israelachvili, J. N. *Intermolecular and Surface Forces*, 3rd ed.; Academic Press: San Diego, 2011.

(2) Evans, D. F.; Wennerstrom, H. *The Colloidal Domain: Where Physics, Chemistry, Biology, and Technology Meet*; Wiley-VCH: New York, 2001.

(3) Mukherjee, K.; Moulik, S. P.; Mukherjee, D. C. Thermodynamics of micellization of aerosol OT in polar and nonpolar-solvents - a calorimetric study. *Langmuir* **1993**, *9*, 1727−1730.

(4) Willard, D. M.; Riter, R. E.; Levinger, N. E. Dynamics of polar solvation in lecithin/water/cyclohexane reverse micelles. *J. Am. Chem. Soc.* **1998**, *120*, 4151−4160.

(5) Dutt, G. B. Does the onset of water droplet formation alter the microenvironment of the hydrophobic probes solubilized in nonionic reverse micelles? *J. Phys. Chem. B* **2004**, *108*, 7944−7949.

(6) Shrestha, L. K.; Shrestha, R. G.; Aramaki, K. Intrinsic parameters for the structure control of nonionic reverse micelles in styrene: SAXS and rheometry studies. *Langmuir* **2011**, *27*, 5862−5873.

(7) Shrestha, L. K.; Yamamoto, M.; Arima, S.; Aramaki, K. Charge-free reverse wormlike micelles in nonaqueous media. *Langmuir* **2011**, *27*, 2340−2348.

(8) Lee, H.-Y.; Diehn, K. K.; Sun, K.; Chen, T.; Raghavan, S. R. Reversible photorheological fluids based on spiropyran-doped reverse micelles. *J. Am. Chem. Soc.* **2011**, *133*, 8461−8463.

(9) Lee, H.-Y.; Diehn, K. K.; Ko, S. W.; Tung, S.-H.; Raghavan, S. R. Can simple salts influence self-assembly in oil? Multivalent cations as efficient gelators of lecithin organosols. *Langmuir* **2010**, *26*, 13831−13838.

(10) Tung, S.-H.; Lee, H.-Y.; Raghavan, S. R. A facile route for creating "reverse" vesicles: insights into "reverse" self-assembly in organic liquids. *J. Am. Chem. Soc.* **2008**, *130*, 8813−8817.

(11) Shrestha, L. K.; Sato, T.; Dulle, M.; Glatter, O.; Aramaki, K. Effect of lipophilic tail architecture and solvent engineering on the structure of trehalose-based nonionic surfactant reverse micelles. *J. Phys. Chem. B* **2010**, *114*, 12008−12017.

(12) Shrestha, L. K.; Shrestha, R. G.; Abe, M.; Ariga, K. Reverse micelle microstructural transformations induced by oil and water. *Soft Matter* **2011**, *7*, 10017−10024.

(13) Berret, J. F.; Appell, J.; Porte, G. Linear rheology of entangled wormlike micelles. *Langmuir* **1993**, *9*, 2851−2854.

(14) Dreiss, C. A. Wormlike micelles: where do we stand? Recent developments, linear rheology and scattering techniques. *Soft Matter* **2007**, *3*, 956−970.

(15) Luisi, P. L.; Scartazzini, R.; Haering, G.; Schurtenberger, P. Organogels from water-in-oil microemulsions. *Colloid Polym. Sci.* **1990**, *268*, 356−374.

(16) Scartazzini, R.; Luisi, P. L. Organogels from lecithins. *J. Phys. Chem.* **1988**, *92*, 829−833.

(17) Schurtenberger, P.; Magid, L. J.; King, S. M.; Lindner, P. Cylindrical structure and flexibility of polymer-like lecithin reverse micelles. *J. Phys. Chem.* **1991**, *95*, 4173−4176.

(18) Schurtenberger, P.; Scartazzini, R.; Luisi, P. L. Viscoelastic properties of polymer-like reverse micelles. *Rheol. Acta* **1989**, *28*, 372−381.

(19) Schurtenberger, P.; Scartazzini, R.; Magid, L. J.; Leser, M. E.; Luisi, P. L. Structural and dynamic properties of polymer-like reverse micelles. *J. Phys. Chem.* **1990**, *94*, 3695−3701.

(20) Shchipunov, Y. A. Lecithin organogel - a micellar system with unique properties. *Colloids Surf., A* **2001**, *183*, 541−554.

(21) Tung, S. H.; Huang, Y. E.; Raghavan, S. R. A new reverse wormlike micellar system: mixtures of bile salt and lecithin in organic liquids. *J. Am. Chem. Soc.* **2006**, *128*, 5751−5756.

(22) Shchipunov, Y. A.; Shumilina, E. V. Lecithin bridging by hydrogen-bonds in the organogel. *Mater. Sci. Eng., C* **1995**, *3*, 43−50.

(23) Tung, S. H.; Huang, Y. E.; Raghavan, S. R. Contrasting effects of temperature on the rheology of normal and reverse wormlike micelles. *Langmuir* **2007**, *23*, 372−376.

(24) Tung, S.-H.; Raghavan, S. R. Strain-stiffening response in transient networks formed by reverse wormlike micelles. *Langmuir* **2008**, *24*, 8405−8408.

(25) Hashizaki, K.; Taguchi, H.; Saito, Y. New lecithin organogels with sugars of RNA and DNA. *Chem. Lett.* **2009**, *38*, 1036−1037.

(26) Hashizaki, K.; Sakanishi, Y.; Yako, S.; Tsusaka, H.; Imai, M.; Taguchi, H.; Saito, Y. New lecithin organogels from lecithin/polyglycerol/oil systems. *J. Oleo Sci.* **2012**, *61*, 267−275.

(27) Hashizaki, K.; Watanabe, N.; Imai, M.; Taguchi, H.; Saito, Y. Possibility of vitamin c to induce the formation of lecithin organogel. *Chem. Lett.* **2012**, *41*, 427−429.

(28) Hashizaki, K.; Taguchi, H.; Saito, Y. A novel reverse worm-like micelle from a lecithin/sucrose fatty acid ester/oil system. *Colloid Polym. Sci.* **2009**, *287*, 1099−1105.

(29) Hofmann, A. F.; Small, D. M. Detergent properties of bile salts - correlation with physiological function. *Annu. Rev. Med.* **1967**, *18*, 333−376.

(30) Carey, M. C.; Small, D. M. Characteristics of mixed micellar solutions with particular reference to bile. *Am. J. Med.* **1970**, *49*, 590−608.

(31) Elsayed, M. M. A.; Cevc, G. The vesicle-to-micelle transformation of phospholipid-cholate mixed aggregates: a state of the art analysis including membrane curvature effects. *Biochim. Biophys. Acta, Biomembr.* **2011**, *1808*, 140−153.

(32) Fahey, D. A.; Carey, M. C.; Donovan, J. M. Bile acid/phosphatidylcholine interactions in mixed monomolecular layers - differences in condensation effects but not interfacial orientation between hydrophobic and hydrophilic bile-acid species. *Biochemistry* **1995**, *34*, 10886−10897.

(33) Heuman, D. M. Distribution of mixtures of bile salt taurine conjugates between lecithin-cholesterol vesicles and aqueous media: An empirical model. *J. Lipid Res.* **1997**, *38*, 1217−1228.

(34) Ollila, F.; Slotte, J. P. A thermodynamic study of bile salt interactions with phosphatidylcholine and sphingomyelin unilamellar vesicles. *Langmuir* **2001**, *17*, 2835−2840.

(35) Cohen, D. E.; Thurston, G. M.; Chamberlin, R. A.; Benedek, G. B.; Carey, M. C. Laser light scattering evidence for a common

wormlike growth structure of mixed micelles in bile salt- and straight-chain detergent-phosphatidylcholine aqueous systems: relevance to the micellar structure of bile. *Biochemistry* **1998**, *37*, 14798−14814.
(36) Hjelm, R. P.; Thiyagarajan, P.; Alkanonyuksel, H. Organization of phosphatidylcholine and bile-salt in rodlike mixed micelles. *J. Phys. Chem.* **1992**, *96*, 8653−8661.
(37) Madenci, D.; Salonen, A.; Schurtenberger, P.; Pedersen, J. S.; Egelhaaf, S. U. Simple model for the growth behaviour of mixed lecithin-bile salt micelles. *Phys. Chem. Chem. Phys.* **2011**, *13*, 3171−3178.
(38) Nichols, J. W.; Ozarowski, J. Sizing of lecithin-bile salt mixed micelles by size-exclusion high-performance liquid-chromatography. *Biochemistry* **1990**, *29*, 4600−4606.
(39) Jeng, U. S.; Su, C. H.; Su, C. J.; Liao, K. F.; Chuang, W. T.; Lai, Y. H.; Chang, J. W.; Chen, Y. J.; Huang, Y. S.; Lee, M. T.; Yu, K. L.; Lin, J. M.; Liu, D. G.; Chang, C. F.; Liu, C. Y.; Chang, C. H.; Liang, K. S. A small/wide-angle X-ray scattering instrument for structural characterization of air-liquid interfaces, thin films and bulk specimens. *J. Appl. Crystallogr.* **2010**, *43*, 110−121.
(40) Kline, S. R. Reduction and analysis of SANS and USANS data using IGOR Pro. *J. Appl. Crystallogr.* **2006**, *39*, 895−900.
(41) Pedersen, J. S. Analysis of small-angle scattering data from colloids and polymer solutions: modeling and least-squares fitting. *Adv. Colloid Interface Sci.* **1997**, *70*, 171−210.
(42) Pedersen, J. S.; Schurtenberger, P. Scattering functions of semiflexible polymers with and without excluded volume effects. *Macromolecules* **1996**, *29*, 7602−7612.
(43) Chen, W. R.; Butler, P. D.; Magid, L. J. Incorporating intermicellar interactions in the fitting of SANS data from cationic wormlike micelles. *Langmuir* **2006**, *22*, 6539−6548.
(44) Cates, M. E.; Candau, S. J. Statics and dynamics of worm-like surfactant micelles. *J. Phys.: Condens. Matter* **1990**, *2*, 6869−6892.
(45) Shervani, Z.; Jain, T. K.; Maitra, A. Nonconventional lecithin gels in hydrocarbon oils. *Colloid Polym. Sci.* **1991**, *269*, 720−726.
(46) Shumilina, E. V.; Khromova, Y. L.; Shchipunov, Y. A. A study of the structure of lecithin organic gels by Fourier transform IR spectroscopy. *Russ. J. Phys. Chem.* **2000**, *74*, 1083−1092.
(47) Max, J.-J.; Chapados, C. Infrared spectroscopy of acetone-hexane liquid mixtures. *J. Chem. Phys.* **2007**, *126*, 154511.
(48) Max, J. J.; Chapados, C. Infrared spectroscopy of acetone-methanol liquid mixtures: hydrogen bond network. *J. Chem. Phys.* **2005**, *122*, 014504.
(49) Cosgrove, T. *Colloid Science: Principles, Methods and Applications*, 2nd ed.; Wiley: Chichester, U.K., 2010.
(50) Shchipunov, Y. A.; Hoffmann, H. Growth, branching, and local ordering of lecithin polymer-like micelles. *Langmuir* **1998**, *14*, 6350−6360.